Journal of Organometallic Chemistry, *459* (1993) 271–281

JOM 23843

Reactions of $[Et_3NH][(\mu\text{-}CO)(\mu\text{-}RS)Fe_2(CO)_6]$ complexes with thiazolyl-, oxazolyl- and imidazoyl-mercurials: a route to $Fe_2(CO)_6$ complexes containing an η^1,η^2-C=N bridge *

Dietmar Seyferth, Lea L. Anderson and William M. Davis

Department of Chemistry, Massachusetts Institute of Technology, Cambridge, MA 02139 (USA)

(Received March 23, 1993)

Abstract

The reaction of complexes of type $[Et_3NH][(\mu\text{-}CO)(\mu\text{-}RS)Fe_2(CO)_6]$ with thiazolyl-, oxazolyl- and N-methylimidazolylmercurials gave products of type in moderate yield, as well as $(\mu\text{-}RS)_2Fe_2(CO)_6$ and elemental mercury. The crystal structure of **13b** (Z = S, R = Et, R^1 = H) is described: space group $P\bar{1}$ (No. 2), a = 9.3478(6) Å, b = 11.4594(6) Å, c = 8.1005(4) Å, α = 97.511(5)°, β = 108.221(5)°, γ = 71.516(5)°, Z = 2, R = 0.060, R_W = 0.064 for 2552 observed reflections.

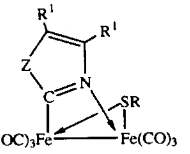

(Z = S, O, CH_3-N)

---

1. Introduction

In a recent publication [1] we reported reactions of $[Et_3NH][(\mu\text{-}CO)(\mu\text{-}RS)Fe_2(CO)_6]$ complexes with furyl-, thienyl- and N-methylpyrrolylmercurials. The reactions with the furyl- and thienylmercurials gave products of type **1**, while di-2-(N-methylpyrrolyl)mercury reacted to give **2**. This chemistry has been extended to include thiazolyl-, oxazolyl- and imidazolylmercurials. These are of interest since their reactions with the $[Et_3NH][(\mu\text{-}CO)(\mu\text{-}RS)Fe_2(CO)_6]$ complexes could give as products neutral $Fe_2(CO)_6$ complexes in which the organic ligand bridges the Fe–Fe unit via its C=N or its C=C moiety or, possibly, in some other manner.

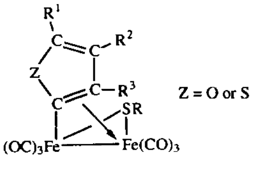

1

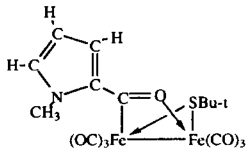

2

Many examples of transition metal complexes with thiazolyl and imidazolyl ligands have been reported. Several involve coordination of the heterocycle to the metal through the carbon atom located between the two hetero-atoms, giving a polarized carbene complex as in **3** and **4** (see refs. 2 and 3 respectively).

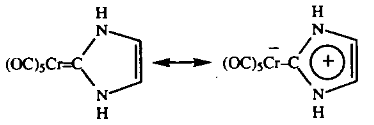

3

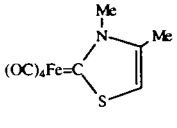

4

Other C-bonded complexes are known: **5** and **6** [4]. Coordination of such heterocycles through nitrogen also has been reported [5], as in **7** [5a] and **8** [5b]. The reaction of $Os_3(CO)_{10}(CH_3CN)_2$ with various imida-

---

Correspondence to: Prof. Dr. D. Seyferth.

* Dedicated, with our very best wishes, to Professor E.O. Fischer on the occasion of his 75th birthday.

0022-328X/93/$6.00

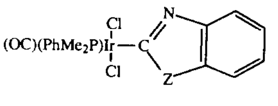

5 (Z = O, S)

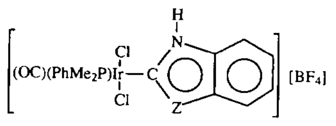

6 (Z = O, S)

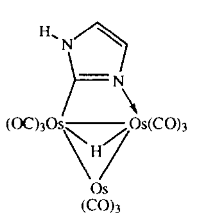

11

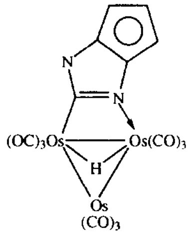

12

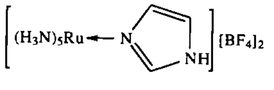

7

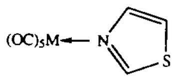

8 (M = Cr, Mo, W)

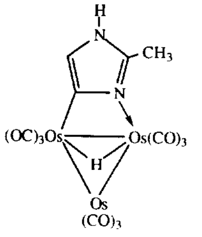

9

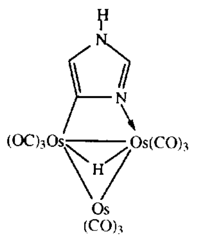

10

zoles gave more complex products. With 2-methylimidazole, a single product, **9**, was obtained [6], whose structure was confirmed by an X-ray diffraction study. In contrast, reaction of imidazole itself with the osmium cluster gave two isomeric complexes. The major product was **10** (which was disordered in the crystal due to reversal of bonded C and N atoms) [6]. The minor isomer, on the basis of NMR spectroscopic evidence, was **11**. Benzimidazole reacted to give **12**.

2. Results and discussion

The required mercurials were prepared as shown in eqns. (1) and (2).

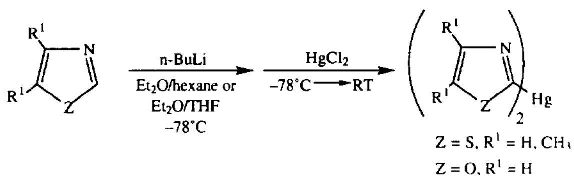

(1)

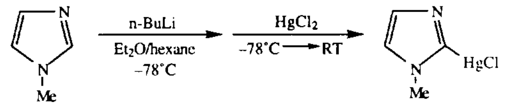

(2)

In their reactions with the $[Et_3NH][(\mu\text{-}CO)(\mu\text{-}RS)Fe_2(CO)_6]$ salts in THF solution, the solid mercurial was added to the iron carbonyl reagent solution against a strong flow of nitrogen. In all cases, immediate gas evolution ensued and a color change from brown-red

TABLE 1. Products of the reactions of $[Et_3NH][(\mu\text{-}CO)(\mu\text{-}RS)Fe_2(CO)_6$ with oxazolyl-, thiazolyl- and N-methylimidazolylmercurials

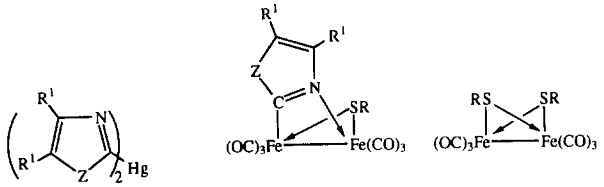

$[Et_3NH][(\mu\text{-}CO\text{-}(\mu\text{-}RS)Fe_2(CO)_6$			13, Yield, %	Yield, %
R	Z	R^1		
^tBu	S	H	**a** 47	26
Et	S	H	**b** 24	59
^tBu	S	CH_3	**c** 37	34
Et	S	CH_3	**d** 13	73
^tBu	O	H	**e** 60	39
Et	O	H	**f** 28	69
^tBu	NCH_3	H [a]	**g** 20	29

[a] Mercurial =

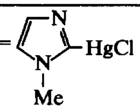

to bright red and the formation of a grey precipitate were observed. (In all prior organomercurial/$[Et_3NH][(\mu\text{-}CO)(\mu\text{-}RS)Fe_2(CO)_6]$ reactions, the latter was found [7] to contain elemental mercury). Thin layer chromatography indicated the formation of two soluble products. Evaporation of volatiles left a red oil or a red solid. Column chromatography of the red residue gave the respective $(\mu\text{-}RS)_2Fe_2(CO)_6$ complex and a product that contained the heterocyclic group, **13**. In some cases, the former was the major product (Table 1) and the yields of the desired product ranged from 13 to 60%. The reactions of $[Et_3NH][(\mu\text{-}CO)(\mu\text{-}PhS)Fe_2(CO)_6]$ with di-2-thiazolylmercury and bis-2-(4,5-dimethylthiazolyl)mercury gave both $(\mu\text{-}PhS)_2Fe_2(CO)_6$ and the desired heterocycle-containing products. However, in both cases, the products were inseparable by column chromatography. The reaction of $[Et_3NH][(\mu\text{-}CO)(\mu\text{-}EtS)Fe_2(CO)_6]$ with 2-chloromercurio-1-methylimidazole gave only $(\mu\text{-}EtS)_2Fe_2(CO)_6$ in 88% yield.

An X-ray diffraction study established the structure of the product of the $[Et_3NH]\{(\mu\text{-}CO)(\mu\text{-}EtS)Fe_2(CO)_6]$/di-2-thiazolylmercury reaction as that shown in Fig. 1. Bond distances and angles are given in Table 2. The thiazolyl ligand is coordinated to the two iron atoms of the $Fe_2(CO)_6$ unit through the nitrogen and carbon atoms of the C=N bond. However, there is a C/N site disorder within the crystal, so that within the unit cell the molecules have two different orientations. For every two molecules with one orientation (A), there is one with the opposite orientation (B). As a result, the bond distances and angles were not completely accurate.

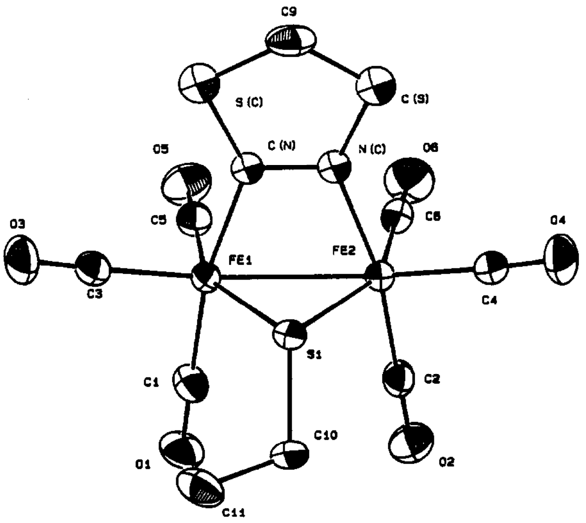

Fig. 1. ORTEP plot for $(\mu\text{-}\overline{C{=}NCH{=}CHS})(\mu\text{-}EtS)Fe_2(CO)_6$, **13b**.

TABLE 2. Intramolecular bond distances (Å) and bond angles (°) for $(\mu\text{-}\overline{C{=}NCH{=}CHS})(\mu\text{-}EtS)Fe_2(CO)_6$ (**13b**) involving the non-hydrogen atoms

Bond lengths			
Fe(1)–Fe(2)	2.609(1)	S(C)–C(N)	1.660(6)
Fe(1)–S(1)	2.261(2)	S(C)–C(9)	1.591(8)
Fe(1)–C(1)	1.807(7)	O(1)–C(1)	1.124(7)
Fe(1)–C(3)	1.797(7)	O(2)–C(2)	1.133(7)
Fe(1)–C(5)	1.802(7)	O(3)–C(3)	1.136(8)
Fe(1)–C(N)	1.976(5)	O(4)–C(4)	1.129(7)
Fe(2)–S(1)	2.266(2)	O(5)–C(5)	1.138(7)
Fe(2)–N(C)	1.983(5)	O(6)–C(6)	1.126(7)
Fe(2)–C(2)	1.782(7)	N(C)–C(N)	1.301(7)
Fe(2)–C(4)	1.809(7)	N(C)–C(S)	1.599(6)
Fe(2)–C(6)	1.798(7)	C(S)–C(9)	1.500(8)
S(1)–C(10)	1.834(6)	C(10)–C(11)	1.51(1)
Bond angles			
Fe(2)–Fe(1)–S(1)	54.89(5)	N(C)–Fe(2)–C(4)	96.1(2)
Fe(2)–Fe(1)–C(1)	98.6(2)	N(C)–Fe(2)–C(6)	89.5(3)
Fe(2)–Fe(1)–C(3)	157.9(2)	C(2)–Fe(2)–C(4)	94.7(3)
Fe(2)–Fe(1)–C(5)	97.1(2)	C(2)–Fe(2)–C(6)	91.8(3)
Fe(2)–Fe(1)–C(N)	70.3(2)	C(4)–Fe(2)–C(6)	98.1(3)
S(1)–Fe(1)–C(1)	92.7(2)	Fe(1)–S(1)–Fe(2)	70.39(5)
S(1)–Fe(1)–C(3)	107.5(2)	Fe(1)–S(1)–C(10)	114.9(2)
S(1)–Fe(1)–C(5)	151.9(2)	Fe(2)–S(1)–C(9)	115.7(2)
S(1)–Fe(1)–C(N)	79.5(2)	C(N)–S(C)–C(9)	94.6(3)
C(1)–Fe(1)–C(3)	95.3(3)	Fe(2)–N(C)–C(N)	108.2(4)
C(1)–Fe(1)–C(5)	92.5(3)	Fe(2)–N(C)–C(S)	136.2(3)
C(1)–Fe(1)–C(N)	168.8(3)	C(N)–N(C)–C(S)	115.4(4)
C(3)–Fe(1)–C(5)	99.4(3)	Fe(1)–C(1)–O(1)	178.4(6)
C(3)–Fe(1)–C(N)	94.7(2)	Fe(2)–C(2)–O(2)	179.4(6)
C(5)–Fe(1)–C(N)	90.7(2)	Fe(1)–C(3)–O(3)	177.4(6)
Fe(1)–Fe(2)–S(1)	54.7(5)	Fe(2)–C(4)–O(4)	176.2(6)
Fe(1)–Fe(2)–N(C)	71.1(1)	Fe(1)–C(5)–O(5)	178.8(6)
Fe(1)–Fe(2)–C(2)	97.7(2)	Fe(2)–C(6)–O(6)	178.2(6)
Fe(1)–Fe(2)–C(4)	160.3(2)	Fe(1)–C(N)–S(C)	135.9(3)
Fe(1)–Fe(2)–C(6)	96.8(2)	Fe(1)–C(N)–N(C)	110.3(4)
S(1)–Fe(2)–N(C)	80.0(2)	S(C)–C(N)–N(C)	113.7(4)
S(1)–Fe(2)–C(2)	93.8(2)	N(C)–C(S)–C(9)	98.1(4)
S(1)–Fe(2)–C(4)	109.3(2)	S(C)–C(9)–C(S)	118.3(4)
S(1)–Fe(2)–C(6)	151.5(2)	S(1)–C(10)–C(11)	110.6(5)
N(C)–Fe(2)–C(2)	168.8(2)		

Estimated standard deviations in the least significant figure are given in parentheses.

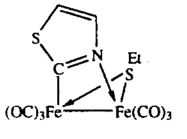

A

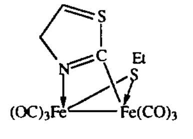

B

In Fig. 1, the atom labels for the ring which are marked with two letters are those which are affected by the disorder. The first label represents the major orientation, the label in parentheses the minor orientation.

The Fe(1)–Fe(2) distance of 2.609(1) Å is within the normal range for an Fe–Fe single bond. The C(N)–N(C) bond distance of 1.301(1), which is normal for a C–N double bond, suggests that the nitrogen atom is coordinated to iron by donation of its lone pair of electrons. If coordination to this iron atom were through the double bond between carbon and nitrogen, one would expect elongation of this bond, as was the case with the π-coordinated C=C double bond of **1**. In addition, the nearly equal bond distances for Fe(1)–C(N) and Fe(2)–N(C) indicate that coordination to iron does not occur through the C=N double bond. Another interesting feature of the molecule is that the atoms Fe(1)–Fe(2)–N(C)–C(N) lie in a nearly perfect plane with a torsion angle of only 0.1°. Thus, the C(N)–N(C) bond is parallel with the Fe(1)–Fe(2) bond. This stands in marked contrast with complex **1** in which the furyl ligand is twisted with respect to the Fe(1)–Fe(2) bond in order to bring C(7) within coordinating distance of Fe(2).

Comparison of the ^{1}H and ^{13}C NMR spectral data for the other complexes of type **13** with those of **13b** provided sufficient evidence to conclude that in all cases the heterocyclic ligand is bonded to the diiron core in a similar manner. Thus, the oxazolyl, thiazolyl and N-methylimidazoyl complexes formed in these reactions all have the structures indicated below.

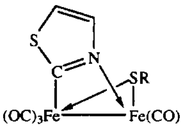

13 a, R = t-Bu
b, R = Et

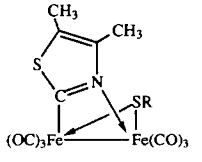

13 c, R = t-Bu
d, R = Et

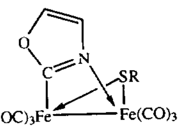

13 e, R = t-Bu
f, R = Et

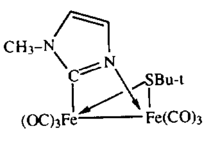

13g

TABLE 3. NMR spectra of **13b**

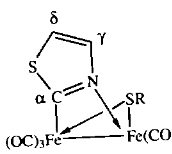

^{1}H NMR spectrum (CDCl$_3$), δ (ppm)	
1.46	t, J = 7.26 Hz, 3H, SCH$_2$CH_3
2.58	q, J = 7.40 Hz, 2H, SCH_2CH$_3$
7.04	AB, J = 3.35 Hz, 2H, C=NCH=CHS
^{13}C NMR spectrum (CDCl$_3$), δ_C (ppm)	
123.36	dd, ^1J = 191.4 Hz, ^2J = 13.8 Hz, C=NCH=C_δHS
143.64	dd, ^1J = 187.6 Hz, ^2J = 8.3 Hz, C=NC_γH=CHS
192.00	s, C_α=NCH=CHS
208.77, 210.04, 212.19	all s, terminal CO's

The ^{1}H NMR spectral data for **13b** are summarized in Table 3. The triplet at 1.46 ppm and the quartet at 2.58 ppm correspond to the protons of the ethyl group of the thiolate ligand. An AB pattern appears at 7.04 ppm with a J(HH) coupling constant of 3.35 Hz. This can be attributed to the olefinic protons of the thiazolyl ligand.

The ^{13}C NMR spectrum also was very useful in identifying the complex. Table 3 summarizes the relevant ^{13}C NMR spectral data for **13b**. As with the furyl-bridged complexes,[1] C_α for **13b** gives rise to a resonance downfield from the analogous resonance for free thiazole due to the σ-coordination of C_α to iron. For complex **13b** this resonance appears at 192.00 ppm, while for free thiazole the corresponding resonance appears at 153.6 ppm [8]. The doublet at 123.36 ppm can be assigned to the carbon atom adjacent to sulfur, C_δ. The other doublet at 143.64 ppm can be assigned to C_γ. These resonances are in close agreement with the analogous resonances for free thiazole at 119.6 and 143.3 ppm, respectively. The J(CH) coupling constants also agree well with the values for thiazole. For **13b** C_δ has J(CH) coupling constant of 191.4 Hz, which is rather close to the value for the olefinic carbon atom adjacent to sulfur of thiazole; J(CH) = 190.6 Hz [9]. Likewise, J(CH) for C_γ of **13b** is 187.6 Hz, while for thiazole the corresponding value is 187.0 Hz. Close inspection of the ^{13}C NMR spectrum for **13b** reveals that these doublets are split further due to long range coupling with the protons of the opposite olefinic carbon atom. This results in each resonance appearing as a doublet of doublets. The resonance of 123.36 ppm has a ^2J(CH) coupling constant of 13.8 Hz, while ^2J(CH) for the remaining resonance at 143.64 ppm is 8.3 Hz.

For the furyl and thienyl complexes [1], the terminal carbonyl groups on iron give rise to a sharp singlet. For complex **13b**, however, three singlets are observed in this region, but close inspection shows that the region is somewhat broadened. In fact, the ^{13}C NMR spectra for all complexes of type **13** show several peaks in this region or a very broad, ill-defined peak. This suggests that the bridging heterocyclic ligand is not fluxional between the two iron centers. A low temperature ^{13}C NMR experiment of **13a** at −50°C produced a spectrum in which the terminal CO region was broadened into a series of peaks. However, all the peaks of the spectrum were broadened at this temperature, which leads to the conclusion that this is probably not due to a slowing down of a fluxional process.

An interesting fact is that for all examples in Table 1 where $R = {}^tBu$, the products were isolated as an inseparable mixture of isomers. The axial isomer is the minor isomer in all cases except for the case of **13e**, in which it is the major isomer. One would expect the equatorial isomer to be major due to steric constraints between the axially oriented thiolate ligand and the bridging heterocycle. In the cases where R = Et, only one isomer of **13** was obtained. The resonances for the protons of these thiolate ligands agree well with the resonances for the equatorial isomer of $(\mu\text{-}EtS)_2Fe_2(CO)_6$. Thus, it can be deduced that only the sterically preferred equatorial isomer is formed.

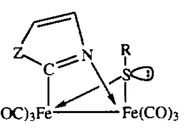

Axial

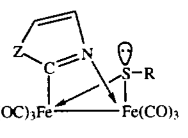

Equatorial

The reaction course in which the heterocycle-containing products are formed very likely is the same as that favored in the formation of the furyl- and thienyl-bridged $Fe_2(CO)_6$ complexes [1]: (1) nucleophilic attack by the $[(\mu\text{-}CO)(\mu\text{-}RS)Fe_2(CO)_6]^-$ anion as an iron-nucleophile at mercury with displacement of chloride or an organic anion (which probably is protonated by Et_3NH^+) to form an intermediate containing an Fe–Hg(Het) bond. (2) Extrusion of elemental mercury, giving an intermediate with an Fe–C bond. (3) Migration of the heterocyclic group from iron to the carbon atom of a C≡O ligand. (4) Decarbonylation of this intermediate and coordination of the N atom, via its lone electron pair, to the other Fe atom, giving the final product. Alternatively, the Fe–C bonded intermediate formed in the mercury extrusion step could react directly with expulsion of CO and coordination of N to the other Fe atom, without formation of an acyl intermediate. A scheme showing this general type of reaction course is shown in ref. 1.

3. Experimental details

3.1. General comments

All reactions were carried out under an atmosphere of prepurified tank nitrogen. Tetrahydrofuran (THF) and diethyl ether were distilled under nitrogen from sodium/benzophenone ketyl and purged with nitrogen prior to use. Triethylamine was distilled under nitrogen from calcium hydride and purged with nitrogen prior to use. Ethyl, t-butyl, and phenyl mercaptans were purged with nitrogen and used without further purification. Mercuric chloride (Alfa) and n-butyllithium (Morton Thiokol) were used as received. Thiazole, 4,5-dimethylthiazole, oxazole, and 1-methylimidazole were purchased from Aldrich and used as received. The 2-lithio-derivatives of 1-methylpyrrole [10], thiazole [11], 4,5-dimethylthiazole [11], and oxazole [12] were prepared according to literature procedures. The lithio-derivative of 1-methylimidazole was prepared in the same manner as 2-lithiothiazole. Triiron dodecacarbonyl was prepared by a literature procedure [13].

The progress of all reactions was monitored by thin-layer chromatography (Baker Flex, Silica Gel 1B-F). Purification by filtration chromatography in which the reaction products were dissolved in a suitable solvent and chromatographed on a bed of Mallinckrodt 100 mesh silicic acid (*ca.* 200 ml) in a 350 ml glass fritted funnel was used. Further purification was achieved by column chromatography with a 450 × 25 mm medium pressure column using Sigma S-0507 230-400 mesh or Aldrich, 60 Å, 230–400 mesh silica gel. In addition, preparative thin layer chromatography plates (EM Science 60 F_{254}, silica gel, 20 × 20 × 0.25 cm) were used as needed. All chromatography was completed without exclusion of atmospheric moisture or oxygen. Solid products were recrystallized at −20°C. All yields are based on Fe unless otherwise indicated.

Solution (NaCl windows) or KBr pellet infrared spectra were obtained using a Perkin-Elmer 1600 Series FTIR instrument. Proton NMR spectra were recorded on a Bruker WM-250 or a Varian XL-300 spectrometer operating at 250 and 300 MHz, respectively. Carbon-13 NMR spectra were recorded on a Varian XL-300 spectrometer operating at 75.4 MHz. Electron impact mass spectra were obtained using a Finnigan-3200 mass spectrometer operating at 70 eV. Masses were correlated using the following isotopes: ^1H, ^{12}C, ^{14}N, ^{16}O, ^{32}S, and ^{56}Fe. Melting points were determined in air on a Büchi melting point apparatus using analytically pure samples and are uncorrected. Microanalyses were performed by Scandinavian Microanalytical Laboratory, Herlev, Denmark.

3.2. X-Ray crystallography

A red prism crystal of $(\mu\text{-}\overline{C{=}NCH{=}CHS})(\mu\text{-}EtS)Fe_2(CO)_6$ (**13b**) (grown from pentane at −20°C) having approximate dimensions of 0.020 × 0.180 × 0.150 mm was mounted on a glass fiber. All measurements were made on an Enraf-Nonius CAD-4 diffractometer with graphite monochromated Mo Kα radiation.

Cell constants and an orientation matrix for data collection, obtained from a least-squares refinement using the setting angles of 25 carefully centered reflections in the range $25.00 < 2\theta < 32.00°$ corresponded to a triclinic cell with dimensions given in Table 4. For $Z = 2$ and F.W. = 424.99, the calculated density is 1.806 g/cm^3. Based on packing considerations, a statistical analysis of intensity distribution, and the successful solution and refinement of the structure, the space group was determined to be $P\bar{1}$ (No. 2).

The data were collected at a temperature of 23 ± 1°C using the ω-2θ scan technique to a maximum 2θ value of 54.9°. Omega scans of several intense reflections, made prior to data collection, had an average width at half-height of 0.22° with a take-off angle of 2.8°. Scans of $(0.80 + 0.35 \tan\theta)°$ were made at speeds ranging from 0.9 to 8.0°/min (in omega). Moving-crystal, moving counter background measurements were made by scanning an additional 25% above and below the scan range. The counter aperture consisted of a variable horizontal slit with a width ranging from 3.0 to 3.5 mm and vertical slit set to 4.0 mm. The diameter of the incident beam collimator was 0.8 mm and the crystal to detector distance was 17.3 cm. For intense reflections an attenuator was automatically inserted in front of the detector.

TABLE 4. Crystal data and intensity collection details for $(\mu\text{-}\overline{\text{C=NCH=CHS}})(\mu\text{-EtS})\text{Fe}_2(\text{CO})_6$ (**13**)

Empirical formula	$\text{C}_{11}\text{H}_7\text{Fe}_2\text{NO}_6\text{S}_2$
Formula weight	424.99
Crystal color, habit	red, prism
Crystal dimension (mm)	0.020 × 0.180 × 0.150
Crystal system	triclinic
No. reflections used for unit cell determination (2θ range)	25 (25.0–32.0°)
Omega scan peak width at half-height	0.22
Lattice parameters	$a = 9.3478(6)$ Å
	$b = 11.4594(6)$ Å
	$c = 8.1005(4)$ Å
	$\alpha = 97.511(5)°$
	$\beta = 108.221(5)°$
	$\gamma = 71.516(5)°$
	$V = 781.2(2)$ Å^3
Space group	$P\bar{1}$ (No. 2)
Z value	2
D_{calc}	1.806 g/cm^3
F_{000}	424
$\mu_{(\text{Mo K}\alpha)}$	21.37 cm^{-1}
Diffractometer	Enraf-Nonius CAD-4
Radiation	Mo Kα ($\lambda = 0.71069$ Å)
Temperature	23°C
Attenuator	Zr foil, (factor = 17.9)
Take-off angle	2.8°C
Detector aperture	3.0–3.5 mm horizontal 4.0 mm vertical
Crystal to detector distance	17.3 cm
Scan type	ω–2θ
Scan rate	0.9 – 8.0°/min (in omega)
Scan width	$(0.80 + 0.35 \tan\theta)°$
$2\theta_{\max}$	54.9°
No. of reflections measured	Total: 3816 Unique: 3560 ($R_{\text{int}} = 0.023$)
Corrections	Lorentz-polarization Secondary extinction (coefficient: 0.16212E-05)

TABLE 5. Structure solution and refinement for $(\mu\text{-}\overline{\text{C=NCH=CHS}})(\mu\text{-EtS})\text{Fe}_2(\text{CO})_6$ (**13b**)

Structure Solution	direct methods
Refinement	Full-matrix least-squares
Function minimized	$\Sigma w(\lvert F_o\rvert - \lvert F_c\rvert)^2$
Least-squares weights	$4F_o^2/\sigma^2(F_o^2)$
p-factor	0.03
Anomalous dispersion	All non-hydrogen atoms
No. observations ($I > 3.00\sigma(I)$)	2552
No. variables	180
Reflection/parameter ratio	14.18
Residuals: R; R_w	0.060; 0.064
Goodness of fit indicator	1.88
Max shift/Error in final cycle	0.00
Maximum peak in final diff. map	0.92 e$^-$/Å^3
Minimum peak in final diff. map	−1.12 e$^-$/Å^3

Of the 3816 reflections which were collected, 3560 were unique ($R_{\text{int}} = 0.023$); equivalent reflections were merged. The intensities of three representative reflections, which were measured after every 60 min of X-ray exposure time, remained constant throughout data collection indicating crystal and electronic stability (no decay correction was applied).

The linear absorption coefficient for Mo Kα is 21.4 cm^{-1}. Azimuthal scans of several reflections indicated no need for an absorption correction. The data were corrected for Lorentz and polarization effects. A correction for secondary extinctions was applied (coefficient = 0.16212×10^{-5}).

The structure solution and refinement were complicated by the discovery of site disorder of the thiazole ring. The model for the disorder is as a 2 : 1 occupancy for the SCNC portion. For every two molecules in one orientation there is one in the opposite. There is absolutely no question as to which portion of the ring is bridging the two iron atoms: it is CN bridging. As a result the disordered atoms were not refined anisotropically.

The structure was solved by direct methods [14*]. The non-hydrogen atoms were refined either anisotropically or isotropically. The final cycle of full-matrix least-squares refinement [15*] was based on 2552 observed reflections ($I > 3.00\sigma(I)$) and 180 variable pa-

---

* Reference number with an asterisk indicates a note in the list of references.

TABLE 6. Final positional parameters for $(\mu\text{-}\overline{\mathrm{C{=}NCH{=}CHS}})(\mu\text{-}\mathrm{EtS})\mathrm{Fe_2(CO)_6}$ (**13b**)

Atom	*x*	*y*	*z*	B_{eq}
Fe(1)	−0.7803(1)	−0.21382(8)	0.2538(1)	2.74(4)
Fe(2)	−0.5594(1)	−0.18895(8)	0.1408(1)	2.83(4)
S(1)	−0.6503(2)	−0.3554(1)	0.1881(2)	2.96(7)
S(C)	−0.5079(3)	−0.3447(2)	0.6152(3)	4.45(5)
O(1)	−1.0498(5)	−0.1219(4)	−0.0486(6)	4.9(3)
O(2)	−0.7600(6)	−0.0777(5)	−0.1884(7)	5.7(3)
O(3)	−0.9391(6)	−0.3357(5)	0.4066(7)	6.0(3)
O(4)	−0.2637(6)	−0.2453(5)	0.0497(7)	6.2(3)
O(5)	−0.8410(6)	0.0248(5)	0.4443(6)	5.4(3)
O(6)	−0.5536(7)	0.0533(5)	0.3039(7)	5.8(3)
N(C)	−0.4618(6)	−0.2639(5)	0.3271(7)	3.0(1)
C(1)	−0.9472(7)	−0.1557(6)	0.069(1)	6.3(3)
C(2)	−0.6822(7)	−0.1216(6)	−0.0607(9)	3.5(3)
C(3)	−0.8796(7)	−0.2890(6)	0.3437(9)	3.7(3)
C(4)	−0.3786(8)	−0.2267(6)	0.0809(8)	3.7(3)
C(5)	−0.8162(7)	−0.0680(6)	0.3719(9)	3.7(3)
C(6)	−0.5557(8)	−0.0406(6)	0.2436(8)	3.6(3)
C(N)	−0.5733(6)	−0.2759(5)	0.4226(7)	2.8(1)
C(S)	−0.2866(4)	−0.3200(3)	0.4938(5)	4.30(7)
C(9)	−0.3270(8)	−0.3663(7)	0.6332(9)	4.9(4)
C(10)	−0.7685(7)	−0.3759(6)	−0.1357(8)	3.7(3)
C(11)	−0.8853(9)	−0.4426(7)	−0.139(1)	5.4(4)
H(1)	−0.2439	−0.4083	0.7325	5.6
H(2)	−0.8243	−0.2974	−0.1872	4.5
H(3)	−0.7006	−0.4224	−0.2048	4.5
H(4)	−0.9538	−0.3970	−0.0726	6.3
H(5)	−0.9461	−0.4548	−0.2549	6.3
H(6)	−0.8298	−0.5220	−0.0891	6.3
H(7)	−0.1874	−0.3229	0.4807	5.1
H(8)	−0.5605	−0.3642	0.6865	5.3

Atoms with letter only designations are comprised of 67% of the first element and 33% of the second.

rameters and converged with unweighted and weighted agreement factors of $R = 0.060$ and $R_w = 0.064$.

The standard deviation of an observation of unit weight [16*] was 1.88. The weighting scheme was based on counting statistics and included a factor ($p = 0.03$) to downweight the intense reflections. Plots of $\Sigma w(|F_o| - |F_c|)^2$ *versus* $|F_o|$, reflection order in data collection, $\sin\theta/\lambda$, and various classes of indices showed no unusual trends. The maximum and minimum peaks on the final difference Fourier map corresponded to 0.92 and −1.12 $e^-/Å^3$, respectively.

Neutral atom scattering factors were taken from Cromer and Waber [17]. Anomalous dispersion effects were included in F_{calc} [18]; the values for $\Delta f'$ and $\Delta f''$ were those of Cromer [19]. All calculations were performed using the TEXSAN crystallographic software package of Molecular Structure Corporation [20].

The final positional and isotropic thermal parameters for the non-hydrogen atoms are given in Table 6.

3.3. Preparation of mercurials

3.3.1. Di-2-thiazolylmercury

A 300 ml Schlenk flask equipped with a stir-bar and a rubber septum was degassed by three evacuation/nitrogen-backfill cycles. The system then was charged with 200 ml of diethyl ether and cooled to −78°C using a dry ice/acetone bath. Next, 29 ml (59 mmol, 2.01 M in hexane) of ^{n}BuLi, followed by 5.0 g (59 mmol) of thiazole were added dropwise. The mixture was stirred at −78°C for 10 min, then slowly warmed to −20°C during which time the color became deep yellow-orange. After 15 min the reaction mixture was recooled to −78°C and 8.0 g (30 mmol) of mercuric chloride was added as a solid against a strong flow of nitrogen. The mixture was stirred at −78°C for 2 h, then warmed to room temperature and stirred for an additional 16 h. A light tan precipitate formed which was removed by filtration with suction. The solid was dissolved in boiling ethanol and filtered with suction to remove insoluble material. The volume of solvent was reduced and the solution was placed in a freezer at −20°C to crystallize. The light tan needles which formed yielded 6.4 g (17 mmol, 59%) of di-2-thiazolylmercury, melting range 130–155°C (dec). Anal. Calcd. for $C_6H_4HgN_2S_2$: C, 19.54; H, 1.10; N, 7.60. Found: C, 19.72; H, 1.39; N, 7.45%. ^{1}H NMR ($CDCl_3$, 300 MHz): δ 7.57 (d, $J = 3.51$ Hz, 2H, HgC=NCH=C*H*S), 8.10 (d, $J = 2.94$ Hz, 2H, HgC=NC*H*=CHS). ^{13}C NMR (DMSO, 75.4 MHz): δ 120.96 (dd, $^1J = 189.0$ Hz, $^2J = 8.2$ Hz, HgC=NCH=*C*HS), 143.74 (dd, $^1J = 184.9$ Hz, $^2J = 8.2$ Hz, HgC=N*C*H=CHS), 197.96 (s, Hg*C*=NCH=CHS).

3.3.2. Bis-2-(4,5-dimethylthiazolyl)mercury

A similar procedure was used in the reaction of 2-lithio-4,5-dimethylthiazole (from 44 mmol each of ^{n}BuLi and 4,5-dimethylthiazole) with 22 mmol of $HgCl_2$. The product, a white powder, melting range 144–170°C (dec), was obtained in 49% yield. Anal. Calcd. for $C_{10}H_{12}HgN_2S_2$: C, 28.26; H, 2.85; N, 6.59. Found: C, 28.24; H, 2.88; N, 6.63%. ^{1}H NMR (CD_3OD, 250 MHz): δ 2.27 (s, 6H, HgC=NC(CH_3)=C(CH_3)S), 2.31 (s, 6H, HgC=NC(CH_3)=C(CH_3)S). ^{13}C NMR (DMSO, 75.4 MHz): δ 11.10 (q, 129.0 Hz, HgC=NC(CH_3)=C(CH_3)S), 14.63 (q, $J = 126.3$ Hz, HgC=NC(CH_3)=C(CH_3)S), 126.92 (s, HgC=NC(CH_3)=*C*(CH_3)S), 149.08 (s, HgC=N*C*(CH_3)=C(CH_3)S), 182.82 (s, Hg*C*=NC(CH_3)=C(CH_3)S).

3.3.3. Di-2-oxazolylmercury

Using a similar procedure, the title compound was prepared in 77% yield by reaction of 2-lithiooxazole (from 76 mmol each of n-BuLi and oxazole) with 38 mmol of $HgCl_2$. Melting range, 210–225°C (dec). Anal.

Calcd. for C6H4HgN202: C, 21.40; H, 1.20; N, 8.32. Found: C, 21.13; H, 1.23; N, 8.13%. ~H NMR (DMSO, 250 MHz): ~ 7.29 (s, 2H, HgC=NCH=CHO), 8.26 (s, 2H, HgC=NCH---CHO). 13C NMR (DMSO, 75.4 MHz): 6 125.69 (dd, 1j = 196.6 Hz, 2j = 15.8 Hz, HgC=NCH= CHO), 140.67 (dd, 1j = 207.0 Hz, 2j = 18.7 Hz, HgC= NCH=CHO), 195.59 (s, HgC=NCH=CHO).

3.3.4. 2-Chloromercurio-l-methylimidazole

A similar procedure was used in carrying out the reaction of 2-1ithio-l-methylimidazole (from 40 mmol each of n-BuLi and 1-methylimidazole) and 40 mmol of HgC12 (added in two portions). The grey precipitate which formed was removed by filtration with suction. The solid was dissolved in boiling ethanol and filtered with suction to remove insoluble material. The solvent was removed *in vacuo* to yield 4.15 g (13.1 mmol, 65%) of 2-chloromercuri-l-methylimidazole, as a white powder, melting range = 280-320°C (dec). Anal. Calcd. for C4HsClHgN2: C, 15.15; H, 1.59; N, 8.83. Found: C, 15.90; H, 1.96; N, 8.94%. 1H NMR (CD3OD, 300 MHz): ~53.43 (s, 6H, NCH3), 6.62 (d, J = 1.50 Hz, 2H, HgC=NCH=CHNMe), 6.84 (d, J= 1.52 Hz, 2H, HgC=NCH=CHNMe). 13C NMR (CD3OD, 75.4 MHz): 6 35.28 (q, J = 139.4 Hz, NCH3), 123.34 (dd, 1J= 188.5 Hz, 2j= 14.8 Hz, HgC=NCH=CHNMe), 129.74 (dd, 1j= 189.8 Hz, 2j= 11.1 Hz, HgC-=NCH---CHNMe), 182.82 (s, HgC=NCH=CHNMe).

3.4. Standard in situ preparation of [Et3NH][(tx-CO)(I~-RS)Fe2(CO)6]

A 100 ml Schlenk flask equipped with a rubber septum and a stir-bar was charged with 1.50 g (2.98 mmol) of Fe3(CO)12 and degassed by three evacuation/nitrogen-backfill cycles. The flask then was charged successively with 30 ml of THF, 3.00 mmol of the appropriate thiol, and 0.42 ml (0.30 g, 3.00 mmol) of triethylamine. The mixture was stirred for 15 min at room temperature during which time slow gas evolution and a gradual color change from dark green to brown red-red were observed. The resulting [Et3NH]-[(/z-CO)(/z-RS)Fe2(CO)6], reagent solution then was used *in situ* without further purification.

3.5. Reaction of [Et3NH]I(~-CO)(Ix-tBuS)Fe2(CO)6] with di-2-thiazolylmercury

The standard [EtaNH][(/~-COX/x-tBuS)Fe2(CO)6] reagent solution (2.98 mmol) was prepared at room temperature. Against a strong flow of nitrogen, 1.12 g (3.04 mmol) of di-2-thiazolylmercury was added as a solid. The reaction mixture was stirred for 1 h at room temperature during which time a color change to bright red and the formation of a gray precipitate were observed. TLC indicated the formation of two orange products. The solvent was removed *in vacuo* to yield a red oil which was dissolved in pentane and filtered through a thin pad of silicic acid to remove decomposition products, using pentane as eluant. Further purification of the products was effected by medium pressure column chromatography. Pentane eluted an orange band which gave 0.17 g (0.38 mmol, 26% based on S, a/e:e/e= 1.3)of (//,-tBuS)2Fe2(CO)6, identified by comparison of its 1H NMR spectrum with that of an authentic sample [21]. Continued elution with pentane removed a minor yellow band which was discarded, followed by a red-orange band which yielded 0.62 g (1.40 mmol, 47%) of (/z-C=NCH--CHS)(/~-tBuS)Fe2-(CO)6 (13a) (an inseparable mixture of two isomers) as an air-stable, red-orange solid after recrystallization from pentane, mp 103.0-105.0°C. Anal. Calcd. for C13HllFeENO6S2: C, 34.46; H, 2.45; N, 3.09. Found: C, 34.63; H, 2.51; N, 3.11%. IR (CC14, cm-1): 2960s, 2923s, 1897m, 1872m, 1718s, 1493w, 1472m, 1457m, 1363s, 1302w, 1218m, 1155s, 1133m, 1076m, 1020w, 961m, 880s. Terminal carbonyl region (CCI4, cm-l): 2072vs, 2028vs, 1992vs, 1969vs, 1946sh. IH NMR (CDC13, 300 MHz): 6 1.01 (s, 3.1H, SC(CH3)3, minor isomer), 1.47 (s, 5.9H, SC(CH3)3, major isomer), 7.05 (AB, J= 3.32 Hz, 1.2H, FeC=NCH=CHS, major isomer), 7.07 (AB, J = 3.33 Hz, 0.8H, FeC=NCH=CHS, minor isomer). 13C NMR (CDCI3, 75.4 MHz): 6 33.66 (q, J= 127.9 Hz, SC(Cn3)3, minor isomer), 34.19 (q, J= 127.0 Hz, SC(CH3)3, major isomer), 47.45 (s, SC(CH3)3, minor isomer), 49.52 (s, SC(CH3)3, major isomer), 122.96 (dd, 1j= 189.8 Hz, 2j= 12.0 Hz, FeC=NCH=CHS, minor isomer), 123.38 Hz, (dd, 1j = 193.1 Hz, 2j= 12.0 Hz, FeC=NCH=CHS, major isomer), 143.16 (dd,. 1j= 188.2 Hz, 2j= 8.6 Hz, FeC=NCH=CHS, minor isomer), 143.62 (dd, 1j = 187.6 Hz, 2j=8.7 Hz, FeC=NCH---CHS, major isomer), 192.58 (s, FeC=NCH=CHS, major isomer), 193.57 (s, FeC=NCH=CHS, minor isomer), 207.62, 210.42, 210.53 (all s, terminal CO's). Mass Spectrum (El); *m/z* (relative intensity): 453 (M÷, 6), 425 (M÷- CO, 5), 397 (M÷- 2CO, 10), 369 (M÷- 3CO, 28), 341 (M÷- 4CO, 22), 313 (M÷- 5CO, 24), 285 (M÷- 6CO, 72), 229 (Fe2SH(C=NCH=CHS)+, 100), 202 (Fe2S(SC=N)+, 13), 176 (Fe2S2+, 24), 144 (Fe2S+, 20), 89 (FeSH÷, 3), 85 (C=NCH=CHS÷+ 1H, 13), 56 (Fe÷, 12), 41 (C=NCH÷ + 2H, 29).

3.6. Preparation of other thiazole-derived Fe2(CO)6 complexes

Essentially the same procedure and the same scale that were used in the [Et3NH][(/z-CO)(/x-tBuS)Fe2-(CO)6]/di-2-thiazolylmercury reaction were used in the preparation of the following:

(μ-$\overline{\mathrm{C{=}NCH{=}CHS}}$)(μ-EtS)Fe$_2(CO)_6$ (**13b**) as an air-stable, red-orange, crystalline solid after recrystallization from pentane, mp 65–67°C. Anal. Calcd. for $C_{11}H_7Fe_2NO_6S_2$: C, 31.08; H, 1.66; N, 3.30. Found: C, 31.30; H, 1.84; N, 3.28%. IR (CCl$_4$, cm^{-1}): 2964m, 2929m, 2871w, 1494w, 1454m, 1434w, 1377m, 1360m, 1302m, 1258m, 1133m, 1077m, 1046w, 964s, 881s. Terminal carbonyl region (CCl$_4$, cm^{-1}): 2070vs, 2032vs, 1996vs, 1976vs, 1950m. ^{1}H and ^{13}C NMR are given in Table 2. Mass Spectrum (EI); *m/z* (relative intensity): 425 (M$^+$, 9), 397 (M$^+$ −CO, 10), 369 (M$^+$ − 2CO, 9), 341 (M$^+$ − 3CO, 16), 313 (M$^+$ − 4CO, 9), 285 (M$^+$ − 5CO, 17), 257 (M$^+$ − 6CO, 84), 229 (Fe$_2$SH(C=NCH=CHS)$^+$, 100), 202 (Fe$_2$SC=N$^+$, 92), 144 (Fe$_2$S$^+$, 82), 112 (Fe$_2$$^+$, 18), 88 (FeS$^+$, 14), 85 (C=NCH=CHS$^+$, 16), 56 (Fe$^+$, 63), 43 (unknown, 18).

(μ-σ,π-($\overline{\mathrm{C{=}NCH{=}CHS}}$)(μ-PhS)Fe$_2(CO)_6$, as an inseparable mixture with (μ-PhS)$_2$Fe$_2$(CO)$_6$. ^{1}H NMR (CDCl$_3$, 250 MHz): δ 6.68 (m, 1H, FeC=NCH=C*H*S), 6.84 (s, m, 1H, FeC=NC*H*=CHS), 7.22 (m, 3H, Ph), 7.31 (m, 2H, Ph).

(μ-σ,π-$\overline{\mathrm{C{=}NC(CH_3){=}C(CH_3)S}}$)(μ-^{t}BuS)Fe$_2(CO)_6$ (**13c**) (an inseparable mixture of two isomers), an air-stable, red-orange solid after recrystallization from pentane, mp 111.0–112.0°C. Anal. Calcd. for $C_{15}H_{15}Fe_2NO_6S_2$: C, 37.44; H, 3.15; N, 2.91. Found: C, 37.37; H, 3.25; N, 2.92%. IR (CCl$_4$, cm^{-1}): 2959s, 2923s, 2898m, 2861m, 1718s, 1574w, 1472m, 1456m, 1444m, 1373m, 1364s, 1296m, 1218m, 1155s, 1002m, 951m, 879w. Terminal carbonyl region (CCl$_4$, cm^{-1}): 2066vs, 2026vs, 2002vs, 1946s. ^{1}H NMR 9CDCl$_3$, 250 MHz): δ 1.04 (s, 2.52H, SC(C*H*$_3$)$_3$, minor isomer), 1.45 (s, 6.48H, SC(C*H*$_3$)$_3$, major isomer), 2.02 (s, 1.80H, FeC=NC(CH$_3$)=C(C*H*$_3$)S, major isomer), 2.09 (s, 1.20 H, FeC=NC(CH$_3$)=C(C*H*$_3$)S, minor isomer), 2.12 (s, 1.62 H, FeC=NC(C*H*$_3$)=C(CH$_3$)S, major isomer), 2.16 (s, 1.38H, FeC=NC(C*H*$_3$)=C(CH$_3$)S, minor isomer). ^{13}C NMR (CDCl$_3$, 75.4 MHz): δ 12.00 (q, $J = 129.7$ Hz, FeC=NC(CH$_3$)=C(*C*H$_3$)S, both isomers), 12.22 (q, $J =$ 128.5 Hz, FeC=NC(*C*H$_3$)=C(CH$_3$)S, major isomer), 12.32 (q, $J = 128.7$ Hz, FeC=NC(*C*H$_3$)=C(CH$_3$)S, minor isomer), 31.19 (q, $J = 128.0$ Hz, SC(*C*H$_3$)$_3$, both isomers), 47.24 (s, S*C*(CH$_3$)$_3$, minor isomer), 49.57 (s, S*C*(CH$_3$)$_3$, major isomer), 129.65 (s, FeC=NC(CH$_3$)=*C*(CH$_3$)S, minor isomer), 130.13 (s, FeC=NC(CH$_3$)=*C*(CH$_3$)S, major isomer), 146.38 (s, FeC=N*C*(CH$_3$)=C(CH$_3$)S, minor isomer), 147.21 (s, FeC=N*C*(CH$_3$)=C(CH$_3$)S, major isomer), 188.45 (s, Fe*C*=NC(CH$_3$)=C(CH$_3$), major isomer), 189.00 (s, Fe*C*=NC(CH$_3$)=C(CH$_3$), minor isomer), 210.08–211.62 (broad, terminal *C*O's). Mass Spectrum (EI); *m/z* (relative intensity): 481 (M$^+$, 7), 453 (M$^+$ − CO, 7), 425 (M$^+$ − 2CO, 32), 397 (M$^+$ − 3CO, 15), 369 (M$^+$ − 4CO, 20), 341 (M$^+$ − 5CO, 25), 313 (M$^+$ − 6CO, 80), 257 (Fe$_2$SH(C=NC(Me)=C(Me)S$^+$, 100), 230 (Fe$_2$SH(SC=NCMe)$^+$, 17), 202 (FeSH(C=NC(Me)=C(Me)S)$^+$ + 1H or Fe$_2$S^{t}Bu$^+$ + 1H, 30), 176 (Fe$_2$S$_2$$^+$, 39), 170 (Fe$_2$SC=N$^+$, 22), 144 (Fe$_2S^+$, 15), 113 (C=NC(Me)=C(Me)S$^+$ + 1H, 10), 97 (C=NC(Me)=CS$^+$, 5), 85 (SC=NCMe$^+$, 9), 71 (SC=CH$^+$, 14), 56 (Fe$^+$, 6).

(μ-$\overline{\mathrm{C{=}NC(CH_3){=}C(CH_3)S}}$)(μ-EtS)Fe$_2(CO)_6$ (**13d**) as an air-stable, red-orange solid after recrystallization from pentane, mp 50.0–51.0°C. Anal. Calcd. for $C_{13}H_{11}Fe_2NO_6S_2$: C, 34.46; H, 2.45; N, 3.09. Found: C, 34.62; H, 2.55; N, 3.09%. IR (CCl$_4$, cm^{-1}): 2982m, 2966m, 2926s, 2864w, 1575w, 1446m, 1373s, 1296m, 1258m, 1174w, 1106w, 1046w, 1004s, 953s, 869w. Terminal carbonyl region (CCl$_4$, cm^{-1}): 2067vs, 2026vs, 1990vs, 1971vs, 1947s. ^{1}H NMR (CDCl$_3$, 250 MHz): δ 1.43 (t, $J = 7.34$ Hz, 3H, SCH$_2$C*H*$_3$), 2.03 (s, 3H, FeC=NC(CH$_3$)=C(C*H*$_3$)S), 2.11 (s, 3H, FeC=NC(C*H*$_3$)=C(CH$_3$)S), 2.54 (q, $J = 7.33$ Hz, 2H, SC*H*$_2$CH$_3$). ^{13}C NMR (CDCl$_3$, 75.4 MHz): δ 11.85 (q, $J = 129.6$ Hz, FeC=NC(CH$_3$)=C(*C*H$_3$)S), 12.15 (q, $J =$ 128.4 Hz, FeC=NC(*C*H$_3$)=C(CH$_3$)S), 18.20 (q, $J =$ 128.3 Hz, SCH$_2$*C*H$_3$), 33.65 (t, $J = 141.1$ Hz, S*C*H$_2$CH$_3$), 129.92 (s, FeC=NC(CH$_3$)=*C*(CH$_3$)S), 147.10 (s, FeC=N*C*(CH$_3$)=C(CH$_3$)S), 187.80 (s, Fe*C*=NC(CH$_3$)=C(CH$_3$)S), 208.88, 210.14, 212.06 (all s, terminal *C*O's). Mass Spectrum (EI); *m/z* (relative intensity): 453 (M$^+$, 16), 425 (M$^+$ − CO, 12), 397 (M$^+$ − 2CO, 21), 369 (M$^+$ − 3CO, 35), 341 (M$^+$ − 4CO, 19), 313 (M$^+$ − 5CO, 24), 285 (M$^+$ − 6CO, 76), 257 (Fe$_2$SH(C=NC(Me)=C(Me)S)$^+$, 100), 230 (Fe$_2$SH(SC=NCMe)$^+$, 8), 224 (Fe$_2$SEt(C=NC=C)$^+$ + 1H, 6), 202 (FeSH(C=NC(Me)=C(Me)S$^+$ + 1H, 30), 176 (Fe$_2$S$_2$$^+$, 31), 170 (Fe$_2$SC=N$^+$, 22), 144 (Fe$_2S^+$, 11), 113 (C=NC(Me)=C(Me)S$^+$ + 1H, 3), 85 (SC=NCMe$^+$, 3), 71 (SC=NCH$^+$, 3), 56 (Fe$^+$, 2).

(μ-$\overline{\mathrm{C{=}NC(CH_3){=}C(CH_3)S}}$)(μ-PhS)Fe$_2(CO)_6$, as an inseparable mixture with (μ-PhS)$_2$Fe$_2$(CO)$_6$. ^{1}H NMR (CDCl$_3$, 250 MHz): δ 1.81 (s, 0.8H, FeC=NC(CH$_3$)=C(C*H*$_3$)S, minor isomer), 1.87 (s, 0.8H, FeC=NC(C*H*$_3$)=C(CH$_3$)S, minor isomer), 2.10 (s, 2.2H, FeC=NC(CH$_3$)=C(C*H*$_3$)S, major isomer), 2.15 (s, 2.2H, FeC=NC(C*H*$_3$)=C(CH$_3$)S, major isomer), 7.18 (m, 3H, Ph, both isomers), 7.34 (m, 2H, Ph, both isomers).

3.7. Reaction of [Et$_3$NH][(μ-CO)(μ-^{t}BuS)Fe$_2$(CO)$_6$] with di-2-oxazolylmercury

The standard [Et$_3$NH][(μ-CO)(μ-^{t}BuS)Fe$_2$(CO)$_6$] reagent solution (2.98 mmol) was prepared at room temperature. Against a strong flow of nitrogen, 1.03 g (3.04 mmol) of di-2-oxazolylmercury was added as a solid. An immediate reaction ensued with rapid gas evolution and a color change to red-brown. After the reaction mixture had been stirred for 1 h at room temperature, the color of the solution had changed to bright orange-red and a gray precipitate had formed. TLC indicated the formation of two orange products. The solvent was removed *in vacuo* to yield a red solid which was dissolved in pentane and filtered through a thin pad of silicic acid to remove decomposition products, using pentane as eluant. Further purification of the products was achieved by medium pressure column chromatography. Pentane eluted an orange band which gave 0.26 g (0.58 mmol, 39% based on S, a/e : e/e = 1.4) of $(\mu\text{-}^t\text{BuS})_2\text{Fe}_2(\text{CO})_6$, identified by comparison of its ^{1}H NMR spectrum with that of an authentic sample [21]. Continued elution with pentane removed a red-orange band which yielded 0.78 g (1.79 mmol, 60%) of $(\mu\text{-}\overline{\text{C=NCH=CHO}})(\mu\text{-}^t\text{BuS})\text{Fe}_2(\text{CO})_6$ (**13e**) (an inseparable mixture of two isomers) as an air-stable, red-orange, crystalline solid after recrystallization from pentane, mp 100.0–102.0°C. Anal. Calcd. for $\text{C}_{13}\text{H}_{11}\text{Fe}_2\text{NO}_7\text{S}$: C, 35.73; H, 2.54; N, 3.20. Found: C, 35.88; H, 2.62; N, 3.24%. IR (CCl_4, cm^{-1}): 2968m, 2940m, 2922m, 2896m, 2864w, 1472m, 1454m, 1433m, 1415w, 1364m, 1311m, 1155s, 1122s, 1117s, 1035s, 945m, 910s. Terminal carbonyl region (CCl_4, cm^{-1}): 2074vs, 2032vs, 1988vs, 1978vs, 1955m. ^{1}H NMR (CDCl_3, 250 MHz): δ 1.04 (s, 4.98H, $\text{SC}(\text{C}H_3)_3$, major isomer), 1.47 (s, 4.02H, $\text{SC}(\text{C}H_3)_3$, minor isomer), 6.50 (s, 1H, FeC=NC*H*=CHO, both isomers), 7.50 (s, 0.4H, FeC=NCH=C*H*O, minor isomer), 7.52 (s, 0.6H, FeC=NCH=C*H*O, major isomer). ^{13}C NMR (CDCl_3, 75.4 MHz): δ 33.87 (q, J = 128.1 Hz, $\text{SC}(C\text{H}_3)_3$, major isomer), 34.12 (q, J = 127.0 Hz, $\text{SC}(C\text{H}_3)_3$, minor isomer), 46.98 (s, $\text{S}C(\text{CH}_3)_3$, major isomer), 40.51 (s, $\text{S}C(\text{CH}_3)_3$, minor isomer), 126.24 (dd, ^1J = 193.4 Hz, ^2J = 16.8 Hz, FeC=N*C*H=CHO, major isomer), 126.45 (dd, ^1J = 198.8 Hz, ^2J = 18.6 Hz, FeC=N*C*H=CHO, minor isomer), 143.22 (dd, ^1J = 209.4 Hz, ^2J = 18.0 Hz, FeC=NCH=*C*HO, major isomer), 144.33 (dd, ^1J = 210.6 Hz, ^2J = 19.3 Hz, FeC=NCH=*C*HO, minor isomer), 187.90 (s, Fe*C*=NCH=CHO, minor isomer), 188.08 (s, Fe*C*=NCH=CHO, major isomer), 207.30, 208.66, 209.90, 211.61 (all s, terminal *C*O's). Mass Spectrum (EI); m/z (relative intensity): 437 (M$^+$, 4), 409 (M$^+$ – CO, 10), 381 (M$^+$ – 2CO, 23), 353 (M$^+$ – 3CO, 19), 325 (M$^+$ – 4CO, 14), 297 (M$^+$ – 5CO, 18), 269 (M$^+$ – 6CO, 57), 213 ($\text{Fe}_2\text{SH(C=NCH=CHO)}^+$, 100), 184 ($\text{Fe}_2\text{SH(C=NCH)}^+$, 9), 170 ($\text{Fe}_2\text{S}_2{}^+$, 13), 160 (unknown, 6), 144 (Fe_2S^+, 42), 112 ($\text{Fe}_2{}^+$, 2), 69 (HC=NCH=CHO$^+$, 5), 56 (Fe$^+$, 5), 41 (NCH=CH$^+$ + 1H, 21).

The same procedure and the same scale were used in the preparation of $(\mu\text{-}\overline{\text{C=NCH=CHO}})(\mu\text{-EtS})\text{Fe}_2(\text{CO})_6$ (**13f**) as an air-stable, red-orange, crystalline solid after recrystallization from pentane, mp 59.0–61.0°C. Anal. Calcd. for $\text{C}_{11}\text{H}_7\text{Fe}_2\text{NO}_7\text{S}$: C, 32.30; H, 1.73; N, 3.42. Found: C, 32.45; H, 1.82; N, 3.45%. IR (CCl_4, cm^{-1}): 2982w, 2967w, 2929w, 1452m, 1434m, 1377w, 1312m, 1258m, 1147m, 1126vs, 1110m, 1035s, 946m, 912s. Terminal carbonyl region (CCl_4, cm^{-1}): 2074vs, 2034vs, 1998vs, 1980vs, 1957m. ^{1}H NMR (CDCl_3, 250 MHz): δ 1.45 (t, J = 7.36 Hz, 3H, $\text{SCH}_2\text{C}H_3$), 2.56 (q, J = 7.40 Hz, 2H, $\text{SC}H_2\text{CH}_3$), 6.48 (s, 1H, FeC=NC*H*=CHO), 7.50 (s, 1H, FeC=NCH=C*H*O). ^{13}C NMR (CDCl_3, 75.4 MHz): δ 18.34 (q, J = 128.2 Hz, SCH_2CH_3), 33.67 (t, J = 139.9 Hz, $\text{S}C\text{H}_2\text{CH}_3$), 126.42 (dd, ^1J = 194.8 Hz, ^2J = 16.2 Hz, FeC=N*C*H=CHO), 144.43 (dd, ^1J = 210.6 Hz, ^2J = 16.4 Hz, FeC=NCH=*C*HO), 187.35 (s, Fe*C*=NCH=CHO), 207.85, 209.50, 212.30 (all broad s, terminal *C*O's). Mass Spectrum (EI); m/z (relative intensity): 409 (M$^+$, 3), 381 (M$^+$ – CO, 10), 353 (M$^+$ – 2CO, 19), 325 (M$^+$ – 3CO, 24), 297 (M$^+$ – 4CO, 14), 269 (M$^+$ – 5CO, 23), 241 (M$^+$ – 6CO, 46), 213 ($\text{Fe}_2\text{SH(C=NCH=CHO)}^+$, 100), 184 ($\text{Fe}_2\text{SH(C=NCH)}^+$, 16), 170 ($\text{Fe}_2\text{S}_2{}^+$, 20), 156 (FeS(C=NCH=CHO)$^+$, 5), 144 (Fe_2S^+, 40), 112 ($\text{Fe}_2{}^+$, 4), 85 (FeCHO$^+$, 4), 71 (FeN$^+$ + 1H, 6), 56 (Fe$^+$, 12), 43 (OCH=N$^+$, 6).

3.8. Reaction of $[\text{Et}_3\text{NH}][(\mu\text{-CO})(\mu\text{-}^t\text{BuS})\text{Fe}_2(\text{CO})_6]$ with 2-Chloromercuri-1-methylimidazole

The standard $[\text{Et}_3\text{NH}][(\mu\text{-CO})(\mu\text{-}^t\text{BuS})\text{Fe}_2(\text{CO})_6]$ reagent solution (2.98 mmol) was prepared at room temperature. Against a strong flow of nitrogen, 1.11 g (3.49 mmol) of 2-chloromercuri-1-methylimidazole was added as a solid. The reaction mixture was stirred for 4 h at room temperature during which time a color change to deep red and the formation of a gray precipitate were observed. TLC indicated the formation of two orange products. The solvent was removed *in vacuo* to yield a red solid which was dissolved in pentane/CH_2Cl_2 (3 : 1 v/v) and filtered through a thin pad of silicic acid using pentane as eluant. Further purification of the products was effected by medium pressure column chromatography. Pentane eluted an orange band which gave 0.20 g (0.44 mmol, 29% based on S, a/e : e/e = 1.2) of $(\mu\text{-}^t\text{BuS})_2\text{Fe}_2(\text{CO})_6$, identified by comparison of its ^{1}H NMR spectrum with that of an authentic sample [21]. Continued elution with pentane removed a red-orange band which yielded 0.26 g (0.58 mmol, 20%) of $(\mu\text{-}\overline{\text{C=NCH=CHN}}\text{CH}_3)(\mu\text{-}^t\text{BuS})\text{Fe}_2(\text{CO})_6$ (**13g**) (an inseparable mixture of two isomers) as an air-stable, red solid after recrystallization from pentane, mp 98.5–100.0°C. Anal. Calcd. for $\text{C}_{14}\text{H}_{14}\text{Fe}_2\text{N}_2\text{O}_6\text{S}$: C, 37.36; H, 3.14; N, 6.22. Found: C, 37.53; H, 3.18; N, 6.31%. IR (CCl_4, cm^{-1}): 2966m, 2940m, 2921m, 2896m, 2861w, 1536w, 1526w, 1472m, 1456m, 1446s, 1405m, 1362s, 1289m, 1150s, 1110w, 1076w, 1018w. Terminal carbonyl region (CCl_4, cm^{-1}): 2076vs, 2026vs, 1990vs, 1963vs, 1935m. ^{1}H NMR (CDCl_3, 250 MHz): δ 1.00 (s, 3.33H, $\text{SC}(\text{C}H_3)_3$, minor isomer), 1.47 (s, 5.67H, $\mathrm{SC(C}\mathit{H}_3\mathrm{)_3}$, major isomer), 3.44 (s, 1.62H, $\mathrm{NC}\mathit{H}_3$, major isomer), 3.47 (s, 1.38H, $\mathrm{NC}\mathit{H}_3$, minor isomer), 6.35 (d, $J = 1.81$ Hz, 1H, FeC=NCH=C*H*NMe, both isomers), 6.57 (d, $J = 1.61$ Hz, 1H, FeC=NC*H*=CHNMe, both isomers). ^{13}C NMR ($CDCl_3$, 75.4 MHz): δ 33.80 (q, $J = 139.8$ Hz, $\mathrm{N}\mathit{C}\mathrm{H}_3$, both isomers), 33.82 (q, $J = 128.8$ Hz, $\mathrm{SC(}\mathit{C}\mathrm{H_3)_3}$, minor isomer), 34.21 (q, $J = 126.0$ Hz, $\mathrm{SC(}\mathit{C}\mathrm{H_3)_3}$, major isomer), 46.42 (s, $\mathrm{S}\mathit{C}\mathrm{(CH_3)_3}$, minor isomer), 49.15 (s, $\mathrm{S}\mathit{C}\mathrm{(CH_3)_3}$, major isomer), 123.25 (d, $J = 189.6$ Hz, FeC=NCH=*C*HNMe, minor isomer), 124.29 (d, $J = 190.9$ Hz, FeC=NCH=*C*HNMe, major isomer), 129.24 (d, $J = 187.9$ Hz, FeC=N*C*H=CHNMe, minor isomer), 129.78 (d, $J = 190.6$ Hz, FeC=N*C*H=CHNMe, major isomer), 161.78 (s, Fe*C*=NCH=CHNMe, major isomer), 162.96 (s, Fe*C*=NCH=CHNMe, minor isomer), 208.04, 210.63, 211.38, 212.56 (all s, terminal *C*O's). Mass Spectrum (EI): m/z (relative intensity): 450 (M^+, 13), 422 ($M^+ - CO$, 10), 394 (M^+, 2CO, 11) 366 ($M^+ - 3CO$, 40), 338 ($M^+ - 4CO$, 23), 310 ($M^+ - 5CO$, 22), 282 ($M^+ - 6CO$, 40), 226 ($(Fe_2S(C{=}NCH{=}CHNMe))^+ + 1H$, 100), 198 ($(Fe_2S(NC{=}NCH))^+ + 1H$, 11), 170 ($(Fe_2S(C{=}N))^+$, 17), 144 ($Fe_2S^+$, 41), 82 ($C{=}NCH{=}CHNMe^+ + 1H$, 9), 56 ($Fe^+$, 20), 41 ($HNC{=}N^+$, 78).

3.9. *Reaction of* $[Et_3NH][(\mu\text{-}CO)(\mu\text{-}EtS)Fe_2(CO)_6]$ *with 2-chloromercuri-1-methylimidazole*

The same procedure was followed using the $[Et_3NH][(\mu\text{-}CO)(\mu\text{-}EtS)Fe_2(CO)_6]$ reagent solution (2.98 mmol) and 1.10 g (3.47 mmol) of 2-chloromercuri-1-methylimidazole, added as a solid. TLC indicated the formation of two orange products. The solvent was removed *in vacuo* to yield a red solid which was dissolved in pentane/CH_2Cl_2 (8:1 v/v) and filtered through a thin pad of silicic acid using pentane as eluant. Further purification was achieved by medium pressure column chromatography. Pentane eluted an orange band which gave 0.53 g (1.32 mmol, 88% based on S, a/e:e/e = 2.7) of $(\mu\text{-}EtS)_2Fe_2(CO)_6$ isomers, identified by comparison of the ^{1}H NMR spectrum with that of an authentic sample [22]. No further products were eluted.

Acknowledgement

The authors are grateful to the National Science Foundation for support of this work.

References and notes

1 D. Seyferth, L.A. Anderson, F. Villafañe, M. Cowie and R.W. Hilts, *Organometallics, 11* (1992) 3262.

2 (a) K. Öfele, *J. Organomet. Chem., 12* (1968) P42; (b) K. Öfele, *Angew. Chem., Int. Ed. Engl., 8* (1969) 916.

3 P.J. Fraser, W.R. Roper and F.G.A. Stone, *J. Chem. Soc., Dalton Trans., 50* (1973) C54.

4 P.J. Fraser, W.R. Roper and F.G.A. Stone, *J. Organomet. Chem., 50* (1973) C54.

5 (a) R.J. Sundberg, R.F. Bryan, I.F. Taylor, Jr. and H. Taube, *J. Am. Chem. Soc., 96* (1974) 381; (b) K.H. Pannell, C.C.-Y. Lee, C. Párkányi and R. Redfearn, *Inorg. Chem. Acta, 12* (1987) 127. See also: (c) W.J. Eilbeck, F. Holmes and A.E. Underhill, *J. Chem. Soc. (A)*, (1967) 757; (d) M. Massacesi, G. Ponticelli, V. Maxia and S. Serci, *Spectrochim. Acta, 37A* (1981) 1035; (e) M. Massacesi, *Transition Met. Chem., 6* (1981) 40; (f) M.M. Shoukry, K. Aziz, E.M. Shoukry and S. Hamdallah, *Transition Met. Chem., 14* (1989) 115.

6 (a) J.R. Shapley, D.E. Samkoff, C. Bueno and M.R. Churchill, *Inorg. Chem., 21* (1982) 634; (b) M.R. Churchill and J.R. Missert, *J. Organomet. Chem., 256* (1983) 349.

7 D. Seyferth, C.M. Archer, D.P. Ruschke, M. Cowie and R.W. Hilts, *Organometallics, 10* (1991) 3363.

8 H.-O. Kalinowski, S. Berger and S. Braun, *Carbon-13 NMR Spectroscopy*, John Wiley and Sons, New York, 1988, p. 384.

9 Ref. 8, p. 506.

10 D.A. Shirley, B.H. Gross and P.A. Roussel, *J. Org. Chem., 20* (1955) 225.

11 J. Beraud and J. Metzger, *Bull. Soc. Chim. France*, (1962) 2072.

12 (a) P.A. Jacobi, S.-n. Ueng and D. Carr, *J. Am. Chem. Soc., 44* (1979) 2042; (b) J.C. Hodges, W.C. Patt and C.J. Connolly, *J. Org. Chem., 56* (1991) 449.

13 W. McFarlane and G. Wilkinson, *Inorg. Syn., 8* (1966) 181.

14 Structure solution methods: (a) MITHRIL, an integrated direct methods computer program. *J. Appl. Cryst., 17* (1984) 42, University of Glasgow, UK; (b) DIRDIF, Direct Methods for Difference Structures - an automatic procedure for phase extension and refinement of difference structure factors. P.T. Beurskens, Technical Report 1984/1 Crystallography Laboratory, Toernooiveld, 6525 Ed Nijmegen, Netherlands.

15 Least-squares function minimized: $\Sigma w(|F_o| - |F_c|)^2$ where: $w = 4F_o^2/\sigma^2(F_o^2)$, $\sigma^2(F_o^2) = [S^2(C + R^2B) + (pF_o^2)^2]/\mathrm{Lp}^2$, S = scan rate, C = total integrated peak count, R = ratio of scan time to background counting time, B = total background count, Lp = Lorentz-polarization factor, p = p-factor.

16 Standard deviation of an observation of unit weight: $[w(|F_o| - |F_c|)^2/(N_o - N_v)]^{1/2}$, where N_o = number of observations and N_v = number of variables.

17 D.T. Cromer and J.T. Waber, in J.A. Ibers and W.C. Hamilton (eds.), *International Tables for X-ray Crystallography*, Kynoch Press: Birmingham, UK, 1974, Vol. IV, Table 2.2a.

18 J.A. Ibers and W.C. Hamilton, *Acta Crystallogr., 17* (1964) 781.

19 Ref. 17, Table 2.3.1

20 TEXSAN-TEXRAY Structure Analysis Package, Molecular Structure Corporation, 1985.

21 J.A. De Beer and R.J. Haines, *J. Organomet. Chem., 24* (1970) 757.

22 (a) D. Seyferth, R.S. Henderson and L.-C. Song, *Organometallics, 1* (1982) 125; (b) L.F. Dahl and C.-H. Wei, *Inorg. Chem., 2* (1963) 328; (c) R.S. Henderson, *Ph.D. Dissertation*, Massachusetts Institute of Technology, June 1981, p. 35.